IEEE Open Journal of
Industry Applications

Received 10 March 2020; revised 22 April 2020; accepted 17 May 2020. Date of publication 27 May 2020;
date of current version 9 June 2020. The review of this article was arranged by Editor L. Martirano.

Digital Object Identifier 10.1109/OJIA.2020.2998000

Failure of MV Cable Terminations Due to Supraharmonic Voltages: A Risk Indicator

ÁNGELA ESPÍN-DELGADO (Student Member, IEEE), SHIMI SUDHA LETHA, SARAH K. RÖNNBERG (Senior Member, IEEE), AND MATH H. J. BOLLEN (Fellow, IEEE)

Electric Power Engineering Group, Luleå University of Technology, 971 87 Skellefteå, Sweden

CORRESPONDING AUTHOR: ÁNGELA ESPÍN-DELGADO (e-mail: angela.espin.delgado@ltu.se)

This work was supported by The Swedish Transportation Administration and The Swedish Research Centre.

ABSTRACT This paper addresses the accelerated aging of medium-voltage (MV) cable terminations with resistive stress-grading due to supraharmonics. The paper introduces a simple and quick way to relate the risk of cable termination failure to the characteristics of supraharmonic distortion in the system. The motivation is to give practical recommendations and guidelines to evaluate the risk of failure of cable terminations under the presence of supraharmonics in MV networks. The underlying model relates the heating in the cable termination linearly with the frequency of the voltage applied and proportionally with the square of the magnitude of the voltage. The indicator can be used to decide whether given levels and frequencies of supraharmonics in the MV network represent a risk to cable terminations. The parameters of the cable termination design are not needed for that decision. However, the decision criterion is based on one sample data (Eagle Pass) and more field information is crucial to improve the approach.

INDEX TERMS Dielectric breakdown, dielectric losses, power cable insulation, power quality, power system harmonics, supraharmonics.

I. INTRODUCTION

Supraharmonics or high-frequency distortion are voltage and current waveform distortion in the frequency range 2 to 150 kHz. Supraharmonics have their origin in the active or passive switching of power electronics converters and the transmitters of power line communication (PLC). Some sources of supraharmonics in MV networks are: wind-turbines and parks [1], solar parks [2], static frequency converters (SFC) in railway systems [3], and voltage source converter (VSC)-based transmission controllers [4]. Due to the increasing use of these technologies, during the last decade, supraharmonics in medium-voltage (MV) [2], [3], [5] and low-voltage (LV) [6], [7] grids have received increasing attention. The emission from these sources might have several supraharmonic components in the range 2 to 150 kHz. Authors in [3] report levels up to 400 V at 2 kHz in a 70 kV busbar, and it is shown in [5], [8] that some supraharmonic components can propagate over distances about 16 km in an MV network.

High levels of voltage distortion in the supraharmonic range have been found to create problems in MV installations. In [9], audible noise from electronic devices in an office building is reported to be caused by a converter-fed pump connected to the same MV busbar as the building's installation. Another case is the failure of cable terminations [4]. Previous studies have demonstrated that, even when cable insulation systems have been designed following the standardized recommendations, they might be susceptible to fail when exposed to stresses that were not considered in the design stage [4], [10]. High levels of supraharmonics are likely to be found in MV networks due to high-frequency system resonances triggered by the emission from power electronic devices [10], [11]. Up to date, there are no recommendations on how to quantify and evaluate the impacts of supraharmonics on MV installations.

Cable terminations of resistive/refractive type stress-grading failed during the commissioning stage of the Eagle Pass BTB installation that connects the U.S. and the Mexican transmission grids. Investigation of the problem revealed the existence of high levels of distortion. The distortion was present at a multiple of the switching frequency of the VSC that was amplified due to a local resonance in the network. Voltage distortion with frequency 12.4 kHz (ten times the

TABLE 1. Summary of Case Studies in the Literature

	V_1 (kV)	V_{peak} (kV)	High freq. (kHz)	$V_{SH-\text{peak}}$ (kV)	V_{SH}/V_1 ratio (%)	Duration	Report/surface temp. rise	Single/multiple SH components	V_{rated} (kV_{L-L})
Eagle Pass [4]	10.4	37	1.26, 3.78, 12.4	6	40	Unknown	Failure	Multiple	24
Paulsson et al. [4]	26.2	45	8	8	22	445 h	Failure	Sinus. single	24
Ming et al. [12]	0	14.1	22	14.1	NA	40 min	Hotspots, 9 °C	Sinus. single	Unknown
Banerjee, Jayaram [13]	13	40	7	18.4	100	Unknown	Hotspots, 25 °C	Sinus. single	15
Patel et al. [16]	NA	18.4	3	NA	NA	90 h	Hotspots, 8 °C	PWM	15
Shaker et al. [14]	NA	12	4	NA	NA	1 h	Hotspots, 10 °C	Square-pulse	15
Abbasi et al. [15]	3.2	4.5	NA	NA	NA	43 min	Failure, 194 °C	DC	Unknown
Unpublished	44.5	78	0.71	15	24	< 1 h	Failure	Sinus. single	84

switching frequency of the converter) was found with an amplitude between 13 % and 40 % of the fundamental voltage [4]. Laboratory tests confirmed that the cause of the termination failure was the high supraharmonic distortion [4]. Three cable terminations of the resistive/refractive type failed within 470 h when exposed to a 50 Hz voltage superimposed with high-frequency voltage from 7.5 to 8.5 kHz, with a magnitude which represents 18 % of the total voltage. The study concluded that higher frequencies lead to higher losses in the stress-grading layer; therefore, the higher the frequency of the supraharmonic voltage, the higher the probability of failure of the termination. The time to failure depends on the amplitude and frequency of the supraharmonics, and the ambient temperature.

Further research has been done to understand the process of the failure of cable terminations of the resistive stress-grading type under high-frequency distortion (supraharmonics). According to [12], the surface potential distribution is disturbed under supraharmonic voltages, which results in the appearance of hotspots in the cable termination surface. The hotspots are created because of the flow of capacitive currents that are proportional to the voltage frequency. As shown in [13], the higher the magnitude of the supraharmonic voltage, the higher the increase in the temperature on the cable termination's surface (non-linear relation). Although the maximum voltage peak is significantly increased when supraharmonic voltage is superimposed on the fundamental, the hotspot formation is due mainly to the supraharmonic component. Thus, a waveform with a single high-frequency component can be used independently to test operation cases in which supraharmonics are superimposed to the fundamental. This finding simplifies experimental setups and analysis. In [14] and [15], the modeling of the generated heat in the material due to power losses is studied. High levels of a 710 Hz component were measured in an MV installation, and a cable termination with resistive stress-grading failed though not immediately. The event has not been published. The voltage values are considered as an example of levels that can be present in a real MV installation. A summary of these cases is presented in Table 1.

There are still open questions about the characteristics of supraharmonics and conditions that lead to the failure of cable terminations. Answering these questions is vital for quantifying and evaluating the risks of cable termination failure, but even a first approach on how to apply the available information and identifying red flags is lacking. The interest of industry stakeholders on this issue can be understood since "a likely early cable termination failure is not only a reliability issue but also a loss of asset which translates to financial loss" [16]. Contributions on the topic might also be of interest to standardization committees. Compatibility levels in MV networks are defined for PLC up to 3 kHz in IEC 61000-2-12. Compatibility levels or emission limits for non-intentional emission [6] have not been set. Reference values are available in IEC 61000-2-12 up to 9 kHz, but it is emphasized that further research is needed before their confirmation. Standardization for supraharmonic voltages and currents must be based on reliable information of both existing and expected levels of distortion in the grid, as well as on the behavior of existing equipment when exposed to supraharmonics.

This paper attempts to fill the lack of methods on the quantification and evaluation of the impacts of supraharmonics on MV cable terminations with resistive stress-grading. The approach is: 1) using the models available in the literature to evaluate which characteristics of supraharmonics might lead to insulation failure in cable terminations; 2) summarizing those models into simplified relations between amplitude and frequency of the supraharmonics, and power losses in the cable termination; 3) using those relations to obtain an indicator that can be used for evaluating the impact of supraharmonics on cable terminations. The outcome of this work is to give guidance about which levels of supraharmonics existing in the grid are safe and which might signify a risk of cable termination failure. The main contribution of this paper is the formulation of an indicator that can be used as a rule of thumb for industrial engineers to quantify the risk of cable termination failure due to supraharmonic voltages. The results of the study can be used as a reference for setting limits of supraharmonic emission from MV loads.

II. MODELING THE PHENOMENON

A. CHAIN OF EVENTS RESULTING IN CABLE TERMINATION FAILURE

In cable terminations designs for MV applications, the use of stress-grading materials as part of the insulation system is common due to their low cost and low size solutions [4], [10]. Stress-grading materials are composites whose

electric conductivity is field-dependent, which is achieved using fillers such as silicon carbide (SiC) and zinc oxide varistor material (ZnO-VM) [17]. Resistive stress-grading materials are susceptible to failure due to accelerated aging caused by supraharmonic distortion. Aging happens because resistive stress-grading materials, by design, have inherently high conductivity at supraharmonic frequencies [13]. The latter results in the appearance of hotspots on the surface of the stress-grading layer and the subsequent failure of the insulation system at the cable termination [4], [12].

For the failure of the cable termination due to supraharmonics to occur, the termination has to be of the resistive stress-grading type and certain conditions must hold. These conditions can be visualized as a chain of events and described as follows:

1) High levels of supraharmonic voltages must exist in the MV network. High levels similar to the ones reported in [4] can happen when a system resonance exists and coincides with the frequency of the supraharmonics being injected into the network.
2) The high levels of supraharmonic voltages must affect the cable termination stress-grading material significantly enough to cause power losses, which must be high enough to create hotspots in the stress-grading layer.
3) The temperature on the surface of the hotspots originated by the exposition of the cable termination to high levels of supraharmonics must be high enough and remain long enough to cause degradation of the stress-grading material [16], which will eventually lead to the failure of the cable termination. How high and how long depends on the termination design.

The following is an overview of the models available in the literature that are relevant for studying the phenomenon.

B. RELATIONSHIP BETWEEN THE CHARACTERISTICS OF THE SUPRAHARMONIC DISTORTION AND THE POWER LOSSES IN THE CABLE TERMINATION

Stress-grading in cable terminations is itself an ample and complex topic of study to which experts in insulation systems have been devoted. An in-depth and comprehensive study of the detailed models describing stress-grading in cable terminations is out of the scope of this paper, and the interested reader can refer to specialized publications such as [18]–[22]. A simplified explanation of the functioning of stress-grading in cable terminations is given in this section.

Fig. 1 shows a lateral cross-section view of the cable termination. The equipotential lines of the voltage at high frequency are traced for reference. The function of the stress-grading layer is to control the high electric stress existing at the edge of the semiconductive screen. High electric stresses might lead to partial discharges and subsequent degradation of insulation materials [23]. The stress-grading layer is then ideally designed such that the electric field distributes uniformly over it to avoid high stresses at the edge of the semiconductive screen. This works well at rated power frequency and, in this case, the equipotential lines in Fig. 1 would be equally spaced over the stress-grading layer.

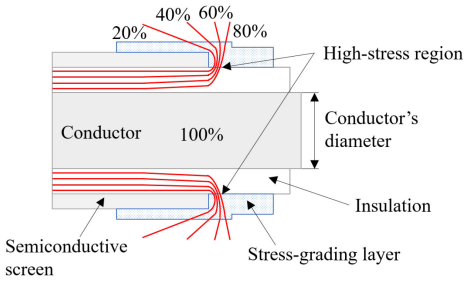

FIGURE 1. Cable termination lateral cross-section view. Example of voltage equipotential lines at high frequencies in a cable termination with resistive stress-grading [4].

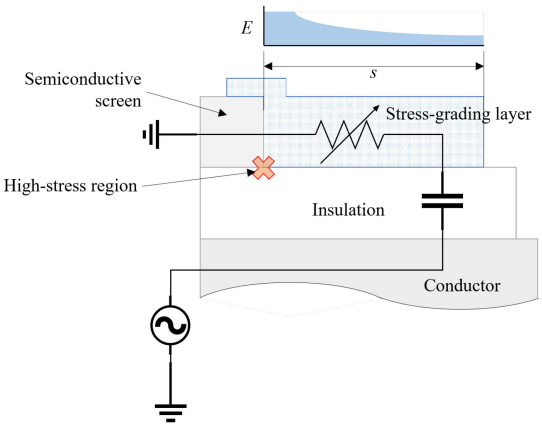

FIGURE 2. Cable termination simplified model. A zoom view from Fig. 1 around the high-stress region.

As exposed to higher frequencies, the stress-grading layer might lose the ability to grade the electric field properly, i.e., the electric field distribution distorts so that high-stress regions are created. For example, high-stress regions can be identified in Fig. 1 because the equipotential lines are concentrated close to the edge of the semiconductive screen. Spatially, the electric field, E, is maximum at the border between the stress-grading layer and the semiconductive screen and decays over the layer with the distance from that border. An example of this behavior is outlined in Fig. 2. Fig. 2 is a zoom view of Fig. 1 around the high-stress region and shows a simplified model of the cable termination. High power losses happen in high-stress regions, which in turn create the hotspots on the surface of the cable termination.

The generated heat inside the cable termination is due to power losses both in the dielectric material of the cable insulation and in the stress-grading layer of the cable termination [10], [12], [23]. The power losses in the dielectric are due to capacitive currents, while the losses in the stress-grading material are resistive.

1) DIELECTRIC LOSSES

As explained in [10], the power dissipated in the insulation material is related to the loss factor, $\tan(\delta)$, the stress voltage, V, and its angular frequency, ω, as follows:

$$P_d = C\tan(\delta)\omega V^2, \tag{1}$$

where C is the total capacitance in the model of Fig. 2, and (1) is valid for sinusoidal stress voltage waveforms. Equivalent forms of (1) are used in [15], [23], [24] as well to model dielectric heating. Models to estimate power dissipation in the dielectric layer of a cable, for arbitrarily waveforms, have been developed in [24].

2) STRESS-GRADING LOSSES

In Fig. 2, the stress-grading layer is modeled by a non-linear resistance, this is because stress-grading materials bear a field-dependent conductivity, $\sigma(E)$. The conductivity is a characteristic unique for each material and increases with the applied electric field so:

$$\sigma(E) = \sigma_0 \exp(kE), \tag{2}$$

where σ_0 and k are positive constants that have been obtained experimentally in previous studies for some materials [17], [20], [23], and E, the electric field. For the development of the risk indicator, (2) is not used. An approximation to the conductivity based on previous research is used instead.

As demonstrated in [18], circuit theory can be used to approximately describe the behavior of the electric field on a non-linear dielectric with characteristic (2) using the concept of the limiting field. The electrical field at the edge of the non-linear dielectric will be limited to a limiting field value, E_{lim}, determined approximately by the condition [18]:

$$\sigma(E_{lim}) = \varepsilon\omega, \tag{3}$$

where ω is the angular frequency of the applied voltage and ε, the dielectric constant of the stress-grading material.

In the context of the impact of supraharmonics on cable terminations, [18] shows that even though the electric field along the stress-grading layer distorts, the electric field has a maximum value that can be predicted by (2) and (3). The maximum conductivity of the material along the layer, which depends linearly on the frequency of the voltage applied, can be predicted by the same equations. This conclusion has been tested by finite element method (FEM) simulations in [23] where good correspondence of results is reported.

As explained in [18], [23], the density of power dissipation in the stress-grading material, P, depends on the electric field, E, and the conductivity, $\sigma(E)$, of the material as follows:

$$P = E^2\sigma(E). \tag{4}$$

The maximum power dissipation P_{max} thus presumably occurs at the limiting electric field. The higher the limiting field, the higher the power dissipation [18]. Thus, the higher the frequency (3), the higher is the power dissipation at the border between the stress-grading layer and the semiconductive screen. However, the average power dissipation, $P_{av} = \int P(E,\sigma)ds$, over the distance s from that border (see Fig. 2), defines the resistive heating in the stress-grading layer [23]. The distribution of the electrical field E as a function of the distance from the edge of the stress-grading layer depends on the characteristics of the material and will not be studied here. It is worth mentioning, though, that the electric potential at a given point over the stress grading layer is related to the electric field so $dV = -E \cdot ds$.

A simplification of the problem is made using the model in Fig. 2. First, the voltage over the stress-grading layer is given by the voltage divider and is proportional to the voltage applied between the conductor and the semiconductive screen, V. Assuming the worst case in which the conductivity of the stress-grading layer is given by (3), the average power dissipation over the stress-grading layer can be expressed as:

$$P_{sg} = aV^2\sigma(E) = aV^2\varepsilon\omega, \tag{5}$$

where a is a factor that accounts for the voltage divider impedance's ratio and the geometry of the stress-grading layer. Simplifying the problem gives an expression for the stress-grading losses similar to that one in (1), in which the losses increase linearly with the frequency and more than linearly with the voltage.

The approximate linear relationship between the stress-grading losses and the frequency in a cable termination has been demonstrated in [17]. The non-linear relationship between the stress-grading losses and the applied voltage is hinted by experimental results in [13], [16], [23]. Further justification for this will be presented in Section III.

C. RELATIONSHIP BETWEEN THE POWER LOSSES AND THE HOTSPOT TEMPERATURE IN THE CABLE TERMINATION

As explained in [13]–[15], the temperature distribution on the stress-grading layer of cable termination can be calculated using the heat equation. In [13], [14], alternative expressions of the heat equation are used for specific purposes where the equation is solved using finite element methods to account for the complexity of the geometry and dynamics of the problem.

The purpose of this paper is to give an indicator based on the characteristics of the supraharmonics and so a relation between temperature and power losses is sought. The heat equation in steady-state is used for this purpose as in [15]:

$$\kappa\nabla^2 T + Q = 0, \tag{6}$$

where T is the temperature, Q is the heat source (power losses), and κ is the thermal conductivity material (assumed constant). In (6), $\nabla^2 T$ is a representation of how steep the temperature distribution is. Eq. (6) has the form of Poisson's equation, which is linear and follows the superposition principle. In this paper, only the effect of the heat source, Q, is accounted. Considering constant temperature at the boundaries of the problem, the temperature rise due to Q is given by T

in (6). As ∇^2 is a linear operator, a change in Q signifies a proportional change in T to maintain the equation.

Detailed thermal models of the cable termination can be consulted in [14], [15].

D. RELATIONSHIP BETWEEN THE HOTSPOT TEMPERATURE AND THE DEGRADATION OF THE CABLE TERMINATION IN TIME DOMAIN

In [16], there is no explicit relationship between hotspot temperature and the degradation of the cable termination. However, exposure of the cable termination to a signal that caused a surface temperature rise of at least 5 °C during approximately 80 hours showed to cause aging in the element. Further experimental information is needed on this matter. A discussion on the time-dependency of the cable aging is presented in Section V-G.

III. DEVELOPMENT OF THE RISK INDICATOR

This paper focuses on the characteristics of supraharmonics that might lead to accelerated aging of cable terminations. The characteristics of supraharmonics considered here are magnitude and frequency. The resulting risk indicator aims to give guidelines on the decision whether a supraharmonic component with certain frequency and magnitude existing in an MV installation might or might not be risky for cable terminations. A detailed model of the phenomenon is out of the scope of this paper. The following assumptions have been made so far:

- The characteristics of the materials cannot be manipulated.
- Except for the conductivity of the stress-grading material, the parameters of the materials, e.g., capacitance and loss factor of the insulation dielectric, are constant with respect to frequency and voltage.
- The conductivity along the stress-grading layer is uniform and depends linearly on the frequency.
- The losses in the cable termination can be modelled by (1) and (5).
- The heat source is given by $Q = P_{sg} + P_d = f(\omega V^2)$. Interpret $f(x)$ as a function of x.
- The system is linear so the superposition principle can be used.

Fig. 3a summarizes experimental data in [23] that shows the behavior of the temperature rise on the surface of a cable termination related to the voltage applied and the frequency of the voltage signal. Sinusoidal waveforms were considered. The points in each curve were used to find a fitted function based on (5) and (6), with the voltage V being the variable and the hotspot temperature rise, $T_{hs} = f(V^2)$, a function of the voltage squared. The fitting exercise resulted in R-square index values around 0.98. The R-square index shows that, in general, the quadratic function represents a good fit to approximate the heating phenomenon.

The heat generated inside the cable termination is given by:

$$Q = P_{sg} + P_d = (a + C\tan(\delta))\,\omega V^2, \tag{7}$$

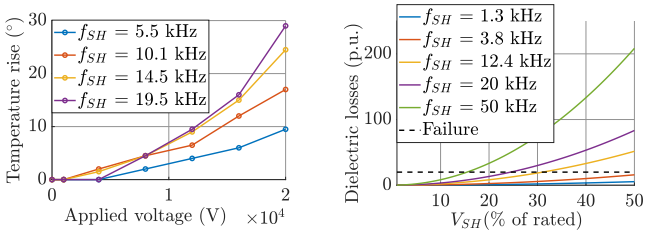

(a) Temperature rise in cable termination surface vs. applied voltage for different frequencies [23].

(b) Power losses as a function of the supraharmonic voltage magnitude for different frequencies of applied distortion.

FIGURE 3. Comparison experimental temperature rise and power losses model curves.

where $(a + C\tan(\delta))$ depends on the design of the cable termination. The power losses inside the cable termination at rated operation are then $Q_{rated} = f(V_{rated}^2 \omega_{rated})$. Eq. (7) can be analyzed for different magnitude, V_{SH}, and angular frequency, ω_{SH}, of voltage supraharmonics. It is useful to represent the losses due to a supraharmonic component, Q_{SH}, as a ratio with respect to the rated losses, Q_{rated}, so:

$$Q_{pu} = \frac{Q_{SH}}{Q_{rated}} = \frac{(a + C\tan(\delta))\,\omega_{SH} V_{SH}^2}{(a + C\tan(\delta))\,\omega_{rated} V_{rated}^2}$$

$$Q_{pu} = \frac{\omega_{SH} V_{SH}^2}{\omega_{rated} V_{rated}^2} = \frac{f_{SH} V_{SH}^2}{f_{rated} V_{rated}^2}, \tag{8}$$

where f and V are frequency and voltage magnitude. This approach was also used in [24]. To decide whether a certain Q_{pu} due to a supraharmonic component might be a risk to the cable termination, the Eagle Pass case [4], where a failure occurred on-site is chosen as the reference. In that case, $V_{rated} = 13.9$ kV RMS and $f_{rated} = 60$ Hz. The conditions when the cable terminations failed in [4] are used as a benchmark, $Q_{pu-fail}$, that is compared against any other Q_{pu} due to supraharmonics in MV. $Q_{pu-fail}$ is the summation of the power losses of supraharmonics at 1.26 kHz, 3.78 kHz and 12.4 kHz with RMS amplitudes 3.12 kV, 0.85 kV and 4.16 kV RMS, respectively. The validity of the summation of power losses is explained in [24] for dielectric losses. The benchmark is then $Q_{pu-fail} \approx 20$, i.e., the cable terminations in Eagle Pass failed when there was sustained heating (during days) due to supraharmonics that created power losses 20 times the power losses at rated operation.

The power losses, Q_{pu}, are visualized as in Fig. 3b as a function of supraharmonic voltage magnitude. $f_{rated} = 60$ Hz and $V_{rated} = 13.9$ kV are considered in (8) for creating the plot. The dashed line represents $Q_{pu-fail}$. The tendencies in Fig. 3b are in accordance to those in [13], [23] and [16].

Assuming that $Q_{pu-fail}$ is exactly the border condition in which Eagle Pass cable termination failed, one can define risk/non-risk regions as: $Q_{pu} < 20$ represents a safe operation, and $Q_{pu} \geq 20$ represents risk of failure. The curve in Fig. 4 shows the pairs voltage magnitude and frequency, (V_{SH}, f_{SH}), that cause as much losses as the failure reference, i.e., it

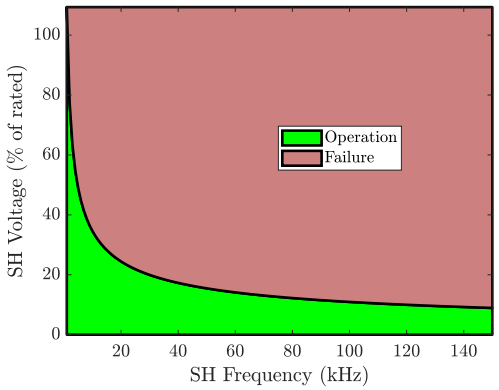

FIGURE 4. Failure border for Eagle Pass case.

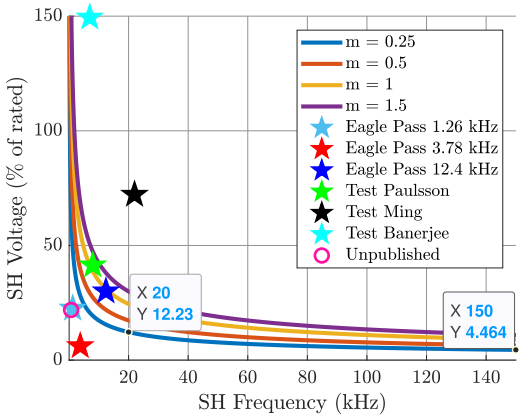

FIGURE 5. Failure borders for different *m* based on Eagle Pass case. The markers represent data of cases available in the literature (Table I).

represents (8) for $Q_{pu} = Q_{pu-fail} = 20$. In Fig. 4, any pair (V_{SH}, f_{SH}) below the curve signifies a safe condition for operation of cable terminations based on Eagle Pass case. Any pair (V_{SH}, f_{SH}) above that curve represents risk of cable terminations failure.

In practice, it is uncertain that $Q_{pu-fail} \approx 20$ for another cable termination or even for the Eagle Pass case: it might be that the power losses that the cable terminations could withstand were lower. An attempt to manage the uncertainty about the value of $Q_{pu_{fail}}$ is to consider a factor m so: $Q_{pu_{fail}} = 20m$. The failure borders are given by supraharmonic voltage magnitude vs. frequency pairs in (8) that meet the condition $Q_{pu} = Q_{pu-fail} = 20m$ for different m. The failure borders considering uncertainty are defined as:

$$Q_{pu-fail} = \frac{f_{SH} V_{SH}^2}{f_{rated} V_{rated}^2} = 20m. \tag{9}$$

This expression can be rearranged as:

$$\frac{V_{SH}}{V_{rated}} = \sqrt{\frac{Q_{pu-fail} f_{rated}}{f_{SH}}} = \sqrt{\frac{20m f_{rated}}{f_{SH}}}. \tag{10}$$

Equation (10) defines a family of curves (failure borders) for a given f_{rated}. Every value of m defines a failure border as shown in Fig. 5. Cable terminations are designed to operate between 48 and 62 Hz [25], i.e., the same termination can operate in a 50 Hz or in a 60 Hz system. For consistency with the previous sections, $f_{rated} = 60$ Hz.

IV. IMPLEMENTATION OF THE RISK INDICATOR

A. NARROWBAND SUPRAHARMONICS

Further simplification of the failure border curves (Fig. 5) can be achieved by picking the results of V_{SH} for $f_{SH} = 20$ and 150 kHz (see the data-boxes in Fig. 5), for $m = 0.25$, 0.5 and 1. This leads to the risk areas in Fig. 6, where m gives an indication of risk. The upper borders of these areas are summarized next:

- Red area ($m > 1$): no upper border.
- Orange area ($0.5 < m < 1$): V_{SH} =24% and 9% for f_{SH} lower and higher than 20 kHz, respectively.

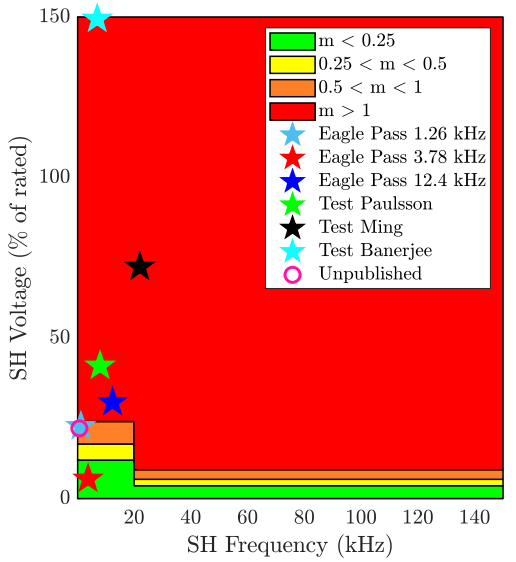

FIGURE 6. Proposed risk areas based on *m* and Eagle Pass case. Test cases superimposed.

- Yellow area ($0.25 < m < 0.5$): V_{SH} =17% and 6% for f_{SH} lower and higher than 20 kHz, respectively.
- Green area ($m < 0.25$): V_{SH} =12% and 4% for f_{SH} lower and higher than 20 kHz, respectively.

The use of these areas depend on how conservative one wants to be. Be reminded that the values are based on the Eagle Pass case.

Data of cases available in the literature are now compared against the failure borders in Fig. 5 and the risk areas in Fig. 6. These data, in the form of pairs (f_{SH}, V_{SH}), are represented by markers in the plots. The three *Eagle Pass* points represent the three supraharmonic components existing in the Eagle Pass failure case; they are considered individually in the plots. In *Test Paulsson* [4], the tested cable terminations failed when a supraharmonic voltage of 5.7 kV RMS at 8 kHz was superimposed to the fundamental frequency. Similarly, the voltages

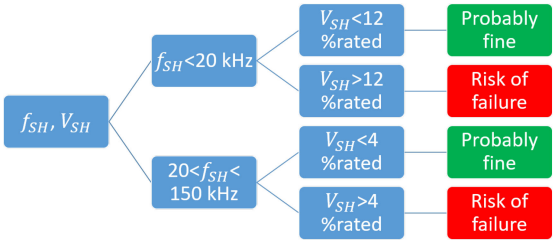

FIGURE 7. Decision algorithm for risk of failure of cable termination due to supraharmonics.

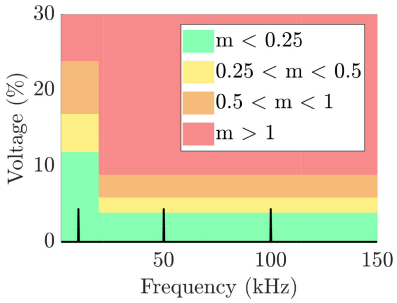

FIGURE 8. Example of a voltage spectrum with more than one supraharmonic component.

and frequencies tested in [12], [13] are also plotted and labeled as *Test Ming* and *Test Banerjee*. For *Test Ming*, $V_{rated} = 24$ kV_{L-L} is assumed. *Unpublished* represents the unpublished cable termination failure case.

In Fig. 5, the *Eagle Pass* 12.4 kHz point falls close to the failure border for $m = 1$, while *Eagle Pass* 1.26 kHz and *Eagle Pass* 3.78 kHz fall in the safe zone below the border for $m = 0.25$. *Test Paulsson* falls on the failure zone of the plane when considering the border corresponding to $m = 1$. *Test Ming* and *Test Banerjee* fall in the failure zone high above the border curve for $m = 1.5$ which leads to think that the conditions would have led the tested cable terminations into failure over time. *Unpublished* falls on the safe operation zone even for $m = 0.25$.

In Fig. 6, most cases fall on the highest risk area defined by $m > 1$. The exceptions are *Eagle Pass* 1.26 kHz and *Unpublished* that fall in the area for $0.5 < m < 1$, and *Eagle Pass* 3.78 kHz that falls in the area for $m < 0.25$. Differences between the approaches in Fig. 5 and 6 are pointed out now.

- *Eagle Pass* 1.26 kHz is classified in Fig. 5 as a safe condition, but it is very close to the highest risk area ($m > 1$) in Fig. 6.
- *Unpublished* falls on the safe operation zone in Fig. 5 but it is classified as a risky condition using the approach in Fig. 6. The conclusion is that the last approach would have been able to predict *Unpublished*.

The idea behind Fig. 6 is to take a rather conservative stance as long as the lack of further information persists. For example, in the case of a single component with the characteristics of *Eagle Pass* 1.26 kHz or *Unpublished*, the recommendation from the authors would be to perform a detailed study. One can be pessimistic and consider that everything that is not inside the green area is a risky condition and needs a closer look. The result is a straightforward decision tree: Fig. 7 shows the algorithm to decide whether supraharmonics, with magnitude V_{SH} and frequency f_{SH}, existing continuously in an MV network can create problems on the cable terminations.

B. MULTIPLE NARROWBAND SUPRAHARMONICS

The literature review conducted in Section I showed no register about systematic experiments to test the impact of multiple narrowband supraharmonic components on cable terminations. The recommendation of the authors on how to treat these cases is to evaluate two steps to identify red flags. The decision is then made based on the worst of the two results.

1) Compare every component individually and make a decision based on the risk areas in Fig. 6 or using Fig. 7.
2) To account for the power loss summation [24], calculate (8) for every supraharmonic component and then sum the results. This can be expressed as:

$$Q_{pu-sum} = \sum_{SH=1}^{N} \frac{V_{SH}^2 f_{SH}}{V_{rated}^2 f_{rated}}, \tag{11}$$

where N is the number of narrowband supraharmonic components to be considered. Make a decision based on the 25% of $Q_{pu-fail}$ in the Eagle Pass case, i.e., $Q_{pu-sum} > 5$ means a risky situation for the integrity of the cable termination.

The spectrum in Fig. 8 is taken as an example. Comparing the components individually to the risk areas reveals that the components at 50 kHz and 100 kHz have magnitudes that might affect the cable termination. Calculating (11) for this spectrum results in $Q_{pu-sum} = 6$.

C. BROADBAND SUPRAHARMONICS

In normal operation, supraharmonics in MV networks usually present a broadband characteristic [3]. Evaluating a spectrum with this characteristic is very challenging due to the lack of information about the impact of broadband supraharmonics on cable terminations and about the lack of consensus about the processing of broadband supraharmonics. It is recommended that these components be treated case by case. In some cases, single-frequency components might appear as broadband components when looked at in the frequency domain. The general recommendation is to group the spectrum using a 2 kHz-bandwidth complying with IEC 61000-4-30 [26] and then apply the approach explained in section IV-B. An example is presented next in Section IV-D.

D. EVALUATING A FREQUENCY SPECTRUM IN THE SUPRAHARMONIC RANGE

A frequency spectrum might reveal both narrowband and broadband supraharmonic components. The recommendations given here are based on the strategies presented in

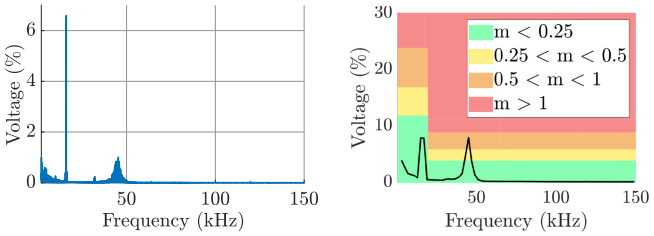

(a) Raw spectrum. 5 Hz resolution. (b) Spectrum with 2 kHz resolution and risk areas.

FIGURE 9. Example of the evaluation of a voltage spectrum with narrow- and broadband supraharmonic components.

Section IV-A and IV-B. The method to evaluate broadband supraharmonics in MV networks is to use an indicator based on (11) and the harmonic power factor proposed in [24]. This is a frequency domain approach and it is assumed that the spectrum of the voltage waveform to evaluate is available and that a suitable pre-processing has been made to take care of the background noise.

First, the grouping bandwidth is 2 kHz complying with IEC 61000-4-30 [26]. Then, the two-step evaluation explained in IV-B is applied. The raw spectrum (5 Hz resolution) in Fig. 9a is taken as an example. The spectrum consists of a narrowband component at 16 kHz and a broadband component around 45 kHz. The spectrum is grouped with a 2 kHz-bandwidth and the first step is to compare it to the risk areas in Fig. 9b. The broadband component surpasses the green area so it is recommended that a detailed study be done to evaluate the impact of it on the cable terminations.

To continue with the second step in IV-B, (11) is updated to account for the range from 2 up to 150 kHz, and the indicator of power losses in the cable termination that might lead to failure due to supraharmonics is defined as:

$$\mathbf{Q_{SH}} = \sum_{B=1}^{74} \frac{V_B^2 f_B}{V_{rated}^2 f_{rated}}, \tag{12}$$

where V_B and f_B are the voltage magnitude and central frequency of a certain frequency band, B. The Eagle Pass case can serve as a reference again, so $\mathbf{Q_{SH-EPass}} \times 0.25 = 20 \times 0.25 = 5$. The indicator for the spectrum in Fig. 9b is $\mathbf{Q_{SH}} = 14$ so even this one is a red flag.

E. STATISTICAL EVALUATION OF THE RISK INDICATOR

According to experimental evidence in [16], the temperature rise in the surface of a cable termination stabilizes approximately 6 hours after constant application of a PWM voltage signal with 3 kHz switching frequency. The power dissipation during short events, e.g., a lightning impulse is not of much consequence as the event is normally too short of causing appreciable heating. However, the steady-state power dissipation must be acceptable for the cable termination not to heat to problematic values [20].

The $\mathbf{Q_{SH}}$ can be evaluated statistically by considering the 99% percentile values calculated every 10 minutes. The values are then aggregated into two-hour periods similar to what is done with the flicker severity indices (Pst and Plt). The evaluation could be performed during a long period, for example, for a whole week. Further work is needed to quantify the loss-of-life associated with the accelerated aging of the cable termination.

V. DISCUSSION AND CONCLUSION

A simple and quick way to relate cable termination failure conditions to the characteristics of supraharmonic distortion present in the system is introduced in this paper. The proposal of such an indicator stood up as a research gap in the literature about cable termination accelerated aging due to supraharmonics. The indicator can be used to give guidelines and recommendations to industry engineers to evaluate the risk of failure of cable terminations under the presence of supraharmonics in MV networks.

A discussion on different aspects of this contribution is presented below.

A. RELEVANT SUPRAHARMONIC CHARACTERISTICS AND MODELING OF THE PHENOMENON

Amplitude and frequency have been identified as attributes of the supraharmonic voltage distortion that give information about their effect on the cable termination power losses and therefore impact their aging. Higher amplitudes and higher frequencies of supraharmonics are related to a higher probability of insulation failure in cable terminations [4], [12], [27]. The model used in this paper considers that the heating in the cable termination is proportional to the frequency of the voltage applied and to the square of the voltage magnitude.

A simplified model of the temperature rise in the cable termination has been used here for developing the risk indicator. Although experimental results published by other research groups show that the simplified model is a good approximation of the phenomenon, further work should be done to confirm that the relationships hold. This holds especially for the case of broadband supraharmonic distortion. An exponential relationship of the temperature with the magnitude of the applied voltage fits also well for some experimental results in the literature [13]. Future work should confirm this relationship and its association with theoretical models that involve both the frequency and magnitude of supraharmonics.

B. EVALUATION OF THE RISK INDICATOR

A risk indicator has been introduced to decide whether given levels and frequencies of supraharmonics in the MV network represent a risk to cable terminations. The model used here allows for a quick evaluation where the parameters of the cable termination design are not needed. However, the decision criterion is based on one sample data (Eagle Pass), and more field information is crucial to improve the approach and to obtain a more accurate decision benchmark.

C. PROCESSING OF SUPRAHARMONICS

The magnitude of broadband components depends on how they are grouped. Therefore, the method of the risk areas introduced in this paper is strongly impacted by the grouping bandwidth used and is recommended to be used mainly for narrowband components. Narrowband components that vary over time might appear as broadband components in the frequency domain. The authors have seen that a 2 kHz-band represents the magnitude of a broadband component better than a 200 Hz-band in some cases; further study is needed to generalize this hypothesis. A 200 Hz-grouping band gives a better possibility to identify narrowband components; it should be used in case of narrowband supraharmonics very close to each other. On the other hand, the $\mathbf{Q_{SH}}$ accounts for the summation of energy, and $\mathbf{Q_{SH}}$ is independent on the grouping bandwidth used. The guidelines given in this section should be used with flexibility based on the specifics of every case.

D. COMPARISON WITH STANDARDIZATION STATUS

The reference levels for PLC (up to 3 kHz) and unwanted narrowband voltages (up to 9 kHz) recommended in IEC 61000-2-12 are within the green area proposed in this paper. The reference level for unwanted broadband voltages (up to 9 kHz) in IEC 61000-2-12 slightly surpasses the green area (about 0.03 percentage points). The treatment recommended by IEC is to use a 200 Hz grouping bandwidth, while in this paper, 2 kHz is advised. Again, further work is needed to decide which one is more suitable.

E. ENVIRONMENTAL TEMPERATURE

The environmental temperature has not been taken into account for the development of the risk indicator. This follows from the aim of the authors to focus on the attributes of the supraharmonics as well as to maintain simplicity. It is uncertain how much the environmental temperature effects the process of degradation of the cable termination in conditions of high supraharmonic distortion [4]. However, studies [28] have demonstrated increased failures of underground cable accessories (cable joints) during summer periods. This might affect electrical systems especially in countries where high temperatures happen during these periods.

F. APPLICABILITY TO OTHER CABLE ACCESSORIES

The extension of this work to cable joints is of interest, as the number of failure of cable joints might be higher than those of cable terminations in some countries [28]. Association of these failure cases with supraharmonics require the study of the methods of field control in cable joints susceptible to non-rated frequency conditions.

G. INTERMITTENT SUPRAHARMONICS EMITTING EQUIPMENT

The emission of supraharmonics depends on the type of equipment and its mode of operation. The stress to which cable terminations are exposed to in case of, e.g., solar generation installations, is not constant. The available information about loss-of-life of the stress-grading type termination due to supraharmonics is summarized as:

- A cable termination continuously exposed to supraharmonics failed within 470 h in [4].
- A cable termination exposed to supraharmonic distortion during 90 h showed significant increment of partial discharge levels after the test in [16].
- The surface temperature of the cable termination in [16] reaches 75% of its maximum after 6 h of continuous exposition to supraharmonics.

The latter indicates that the damage is cumulative and that continuous exposition to supraharmonics for lapses longer than 6 h will accelerate the aging of the materials. The aging caused by short expositions (<6 h) might be negligible compared to the aging caused by longer exposition of the cable termination to supraharmonics.

Methods for the monitoring of the loss-of-life of cable insulation have been developed [29] and are based on the profile of the cable's delivered current and the temperature of the environment. For evaluating supraharmonics, it is the profile of the emission what matters, and the methods already developed for the cable insulation [29] could be extended to the supraharmonics problem.

ACKNOWLEDGMENT

The authors would like to thank The Swedish Transportation Administration and The Swedish Energy Research Centre for supporting this project.

REFERENCES

[1] K. Yang, M. H. J. Bollen, and E. O. A. Larsson, "Aggregation and amplification of wind-turbine harmonic emission in a wind park," *IEEE Trans. Power Del.*, vol. 30, no. 2, pp. 791–799, Apr. 2015.

[2] A. Mohos and J. LadÃąnyi, "Emission measurement of a solar park in the frequency range of 2 to 150 kHz," in *Proc. Int. Symp. Electromagn. Compat. (EMC EUROPE)*, Aug. 2018, pp. 1024–1028.

[3] O. Lennerhag, A. Dernfalk, and P. Nygren, "Supraharmonics in the presence of static frequency converters feeding a 16.7 Hz railway system," in *Proc. Int. Conf. Harmon. Quality Power*, Mar. 2020, pp. 1–6.

[4] L. Paulsson *et al.*, "High-frequency impacts in a converter-based back-to-back tie: The Eagle Pass installation," *IEEE Trans. Power Del.*, vol. 18, no. 4, pp. 1410–1415, Oct. 2003.

[5] A. Novitskiy, S. Schlegel, and D. Westermann, "Analysis of supraharmonic propagation in a MV electrical network," in *Proc. 19th Int. Scientific Conf. Elect. Power Eng.*, May, 2018, pp. 1–6.

[6] S. K. Rönnberg *et al.*, "On waveform distortion in the frequency range of 2 kHz 150 kHz review and research challenges," *Elect. Power Syst. Res.*, vol. 150, pp. 1–10, 2017.

[7] J. Meyer *et al.*, "Overview and classification of interferences in the frequency range 2150 kHz (supraharmonics)," in *Proc. Int. Symp. Power Electron., Elect. Drives, Autom. Motion*, Jun. 2018, pp. 165–170.

[8] A. Novitskiy, S. Schlegel, and D. Westermann, "Measurements and analysis of supraharmonic influences in a MV/LV network containing renewable energy sources," in *Elect. Power Quality Supply Rel. Conf. (PQ) Symp. Elect. Eng. Mechatronics*, Jun. 2019, pp. 1–6.

[9] C. Unger, K. Krager, M. Sonnenschein, and R. Zurowski, "Disturbances due to voltage distortion in the kHz range experiences and mitigation measures," in *Proc. CIRED 18th Int. Conf. Exhib. Elect. Distribution*, Jun. 2005, pp. 1–4.

[10] T. Bengtsson *et al.*, "Repetitive fast voltage stresses-causes and effects," *IEEE Elect. Insul. Mag.*, vol. 25, no. 4, pp. 26–39, Jul. 2009.

[11] S. Sudha-Letha, A. Espín-Delgado, S. Rönnberg, and M. Bollen, "Evaluation of MV/LV network configuration for supraharmonic resonance," unpublished.
[12] Li Ming, F. Sahlen, S. Halen, G. Brosig, and L. Palmqvist, "Impacts of high-frequency voltage on cable-terminations with resistive stress-grading," in *Proc. IEEE Int. Conf. Solid Dielectrics*, Jul. 2004, vol. 1, pp. 300–303.
[13] S. Banerjee and S. H. Jayaram, "Thermal effects of high-frequency voltage on medium voltage cable terminations," in *Proc. IEEE Int. Conf. Solid Dielectrics*, Jul. 2007, pp. 669–672.
[14] Y. O. Shaker, A. H. El-Hag, U. Patel, and S. H. Jayaram, "Thermal modeling of medium voltage cable terminations under square pulses," *IEEE Trans. Dielectrics Elect. Insul.*, vol. 21, no. 3, pp. 932–939, Jun. 2014.
[15] V. Abbasi, S. Hemmati, and M. Moradi, "Effects of stress grading materials properties on the performance of 20-kV cable terminations," *Iranian J. Elect. Electron. Eng.*, vol. 15, no. 1, pp. 56–64, 2019.
[16] U. Patel, S. H. Jayaram, A. El-Hag, and R. Seetahpathy, "MV cable termination failure assessment in the context of increased use of power electronics," in *Proc. Elect. Insulation Conf.*, Jun. 2011, pp. 418–422.
[17] F. P. Espino-Cortes, S. Jayaram, and E. A. Cherney, "Stress grading materials for cable terminations under fast-rise time pulses," *IEEE Trans. Dielectric Elect. Insul.*, vol. 13, no. 2, pp. 430–435, Apr. 2006.
[18] S. A. Boggs, "Theory of a field-limiting dielectric," *IEEE Trans. Power Del.*, vol. 9, no. 3, pp. 1391–1397, Jul. 1994.
[19] T. Christen, L. Donzel, and F. Greuter, "Nonlinear resistive electric field grading part 1: Theory and simulation," *IEEE Elect. Insul. Mag.*, vol. 26, no. 6, pp. 47–59, Nov. 2010.
[20] X. Qi, Z. Zheng, and S. Boggs, "Engineering with nonlinear dielectrics," *IEEE Elect. Insul. Mag.*, vol. 20, no. 6, pp. 27–34, Nov. 2004.
[21] J. Rhyner and M. G. Bou-Diab, "One-dimensional model for nonlinear stress control in cable terminations," *IEEE Trans. Dielectric Elect. Insul.*, vol. 4, no. 6, pp. 785–791, Dec. 1997.
[22] L. Donzel, F. Greuter, and T. Christen, "Nonlinear resistive electric field grading Part 2: Materials and applications," *IEEE Elect. Insul. Mag.*, vol. 27, no. 2, pp. 18–29, Mar. 2011.
[23] S. Banerjee, "A study of high frequency voltage effects in medium voltage cable terminations," Master's thesis, Univ. Waterloo, Waterloo, Canada, 2008.
[24] B. Sonerud, T. Bengtsson, J. Blennow, and S. M. Gubanski, "Dielectric heating in insulating materials subjected to voltage waveforms with high harmonic content," *IEEE Trans. Dielectrics Elect. Insul.*, vol. 16, no. 4, pp. 926–933, Aug. 2009.
[25] *IEEE Standard for Test Procedures and Requirements for Alternating-Current Cable Terminations Used on Shielded Cables Having Laminated Insulation Rated 2.5 kV Through 765 kV or Extruded Insulation Rated 2.5 kV Through 500 kV* IEEE Std 48-2009, Aug. 2009.
[26] *Electromagnetic Compatibility (EMC)-Part 4-30: Testing and Measurement Techniques - Power Quality Measurement methods*, IEC 61000-4-30, 2015.
[27] Q. Nie, Y. X. Zhou, X. L. Xing, and Y. S. Wang, "Breakdown processes of solid composite insulation system with defects under high frequency," in *Proc. Annu. Rep. Conf. Elect. Insul. Dielectric Phenomena*, Oct. 2008, pp. 552–554.
[28] L. Calcara, L. D'Orazio, M. Della Corte, G. Di Filippo, A. Pastore, D. Ricci, and M. Pompili, "Faults evaluation of mv underground cable joints," in *Proc. AEIT Int. Annu. Conf.*, 2019, pp. 1–6.
[29] G. Parise, L. Martirano, L. Parise, L. Gugliermetti, and F. Nardecchia, "A life loss tool for an optimal management in the operation of insulated lv power cables," *IEEE Trans. Ind. Appl.*, vol. 55, no. 1, pp. 167–173, Jan./Feb. 2019.